Andrzej POPENDA

Czestochowa University of Technology

A control strategy of a BLDC motor

***Abstract**. In the paper the control strategy of BLDC motor is proposed. This strategy bases on the electromechanical transformer synchro and voltage source inverter, controlled in the same way as the inverters of AC drives. The pulsations of motor output torque, occurring in the standard control systems of BLDC motor, are eliminated as a consequence of application of the proposed strategy. The magnitude and deformation of motor current as well as the influence of motor load on its angular velocity are also minimized. The results of model-simulation investigations are presented.*

***Streszczenie.** W pracy zaproponowano strategię sterowania silnikiem BLDC, która opiera się na elektromechanicznym przetworniku „synchro" oraz falowniku napięcia sterowanym analogicznie jak falowniki napędów prądu przemiennego. W konsekwencji zastosowania proponowanej strategii wyeliminowano pulsacje momentu elektromagnetycznego silnika, występujące w standardowych układach sterowania silnikiem BLDC. Zminimalizowano również amplitudę i odkształcenia prądu silnika oraz oddziaływanie obciążenia silnika na jego prędkość kątową. Przedstawiono wyniki badań modelowo-symulacyjnych. (**Pewna strategia sterowania silnikiem BLDC**).*

Keywords: BLDC motor, control strategies, synchro and resolver, modelling and simulation.
Słowa kluczowe: silnik BLDC, strategie sterowania, transformatory położenia kątowego, modelowanie i symulacja.

Introduction

Permanent magnet synchronous motors and brushless direct current (BLDC) motors, being a type of permanent magnet synchronous motor, become increasingly popular. The abovementioned motors are commonly used in industry: the examples of industry branches are appliances, automotive, aerospace, consumer, medical, industrial automation equipment and instrumentation [1].

Most BLDC motors include three-phase stator winding connected in star fashion. Each phase winding is constructed with numerous interconnected coils placed in the slots of stator. There are two types of BLDC motors: trapezoidal and sinusoidal [1]. The difference comes from the interconnection of coils in the stator phase windings giving the different types of back electromotive force (EMF), in trapezoidal or sinusoidal fashion, respectively. The analogical classification is applied in relation to the control of BLDC motor electronic commutator. The fashion of back EMF and phase currents of sinusoidal BLDC motor is just sinusoidal, whereas the output torque is smooth, in contrast to the deformed back EMF and phase currents as well as the pulsating output torque of trapezoidal motor, causing the additional vibrations and noise.

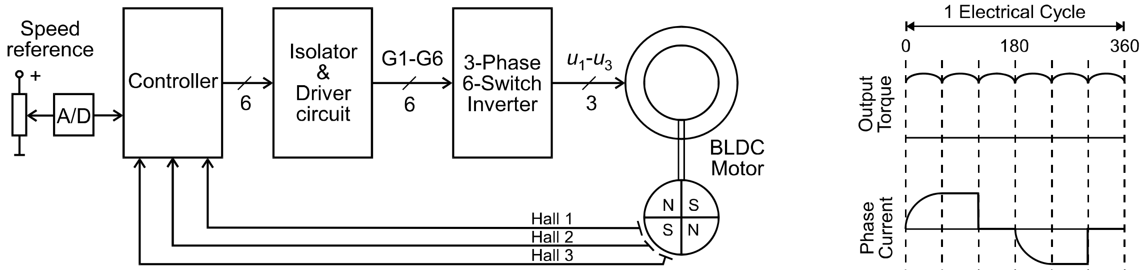

Fig. 1. The block diagram of a standard BLDC motor control system (on the left) and the simplified time changes (without distortion of inverter origin) of output torque and phase current of trapezoidal motor (on the right) [1]

The stator phase windings should be energized in a proper sequence in order to rotate the BLDC motor. The rotor position angle is required in order to determine the windings that have to be energized according to the abovementioned sequence. Three Hall sensors, embedded into the stator on the non-driving end of the motor, allow to determine the rotor position angle in the standard BLDC motor control system (Fig. 1) [1, 3-8]. Optical, magnetic or capacitive encoders as well as electromechanical transducers: resolver or synchro [2] may be used in order to measure a rotor position angle instead of Hall sensors. In contrast to the most popular optical encoders, the resolvers and synchros are resistant to vibrations, strokes, dust and damp as well as permanent operation under high temperature. The lower accuracy of measurement is disadvantage of the abovementioned electromechanical transformers. The rotor of conventional synchro is excited via a pair of slip rings with an alternating carrier voltage u_r. The frequency of this voltage should be at least ten times greater than the frequency corresponding to the maximum rotational speed of motor [2]. The field produced by rotor voltage induces output voltage into each of three stator phase windings. The instantaneous values of stator output voltages may be written as follows:

$$u_{s1} = k_{TR}\, u_r \sin\theta$$

$$u_{s2} = k_{TR}\, u_r \sin(\theta - 120°) \qquad (1)$$

$$u_{s3} = k_{TR}\, u_r \sin(\theta + 120°)$$

where k_{TR} is the transformation ratio and θ is the phase angle of synchro output voltage depending on the rotor position angle γ_m.

Several varieties of brushless synchros are available for applications where conventional commutation with slip rings and brushes is either undesirable or unwanted [2].

Description of the strategy

A control system (Fig. 2) based on the proposed strategy includes the PWM-controlled voltage source inverter, such as the inverters used in converter-fed AC drives with induction motor or synchronous motor. However, an application of feedbacks in the proposed structure causes that rotational speed of BLDC motor is controlled by changes of feeding voltage, whereas rotational speed of induction and synchronous motors is controlled by changes of frequency. In the proposed structure the electromechanical transducer synchro replaced Hall sensors, that are commonly used in order to estimate the rotor position angle of BLDC motor in conventional control systems. A three-phase motor requires a three-phase synchro with the same number of magnet poles [2]. A greater resistance of drive system to the previously described disadvantageous working conditions is the additional good consequence of the abovementioned replacement. The three-phase synchro decoder, including a three-phase synchro, three demodulators (being usually the integrated circuits) and a carrier square wave generator, is shown in Fig. 3. Three demodulators of synchro decoder (one for each modulated synchro output) separate the carrier frequency from the modulation frequency (motor rotation). The three-phase synchro decoder produces three phase-shifted output voltages with magnitude $k_{TR}U_{rm}$, where U_{rm} is magnitude of carrier voltage. In the proposed structure (Fig. 2) the output voltages of synchro decoder are multiplied by u'_{ref} and amplified using voltage source inverter. As the consequence the magnitude of fundamental harmonic of motor phase voltages is equal to $U_m = k_{TR}\, k_{Inv}\, u'_{ref}\, U_{rm}$.

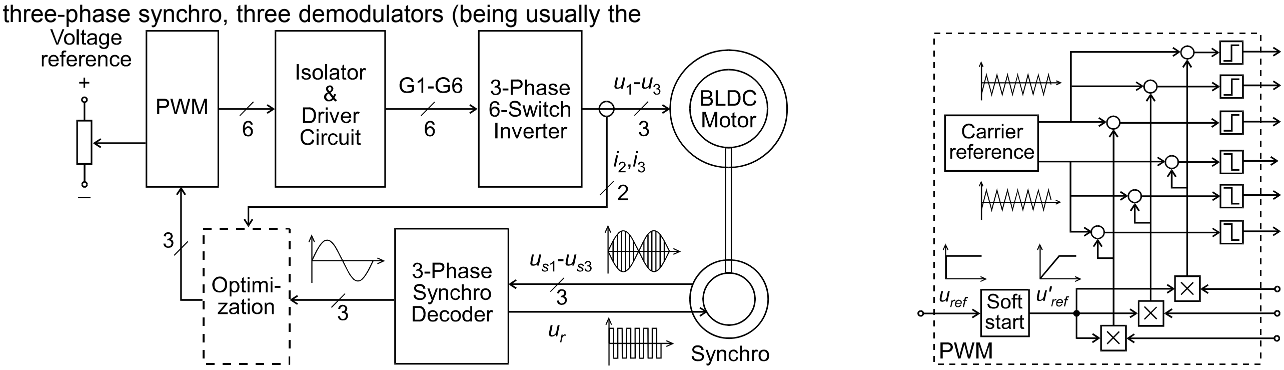

Fig. 2. The block diagrams of: the structure based on the proposed control strategy for BLDC motor (on the left) and the pulse width modulator (PWM) used in the proposed control structure (on the right)

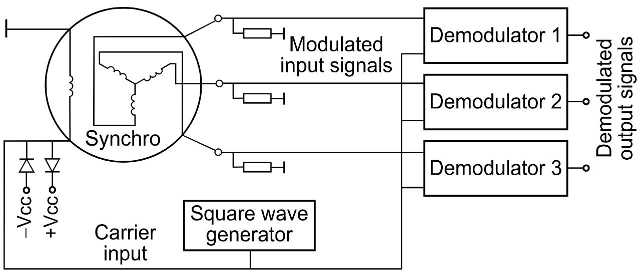

Fig. 3. The three-phase synchro decoder

The dependency between the phase angle θ of synchro output voltage and the BLDC motor rotor position angle γ_m, corresponding with the proper synchronization of the synchro and BLDC motor shafts, is given as follows:

$$\theta = \gamma + 180°, \quad \gamma = p_b \gamma_m \tag{2}$$

where: p_b is number of pole pairs of BLDC motor and synchro. Dependencies between reference frames (coordinate systems) considered in the further parts of the paper, including angles θ and γ, are shown in Fig. 4, where 1,2,3 are the phase coordinates of the stationary three-phase reference frame, 0αβ is the stationary Cartesian coordinate system, 0dq is the rotating Cartesian coordinate system connected to the rotor of BLDC motor. The output voltages of synchro decoder as functions of angle γ are given as follows:

$$\begin{aligned} u_{d1} &= -\,k_{TR}U_{rm}\sin\gamma \\ u_{d2} &= -\,k_{TR}U_{rm}\sin(\gamma - 120°) \\ u_{d3} &= -\,k_{TR}U_{rm}\sin(\gamma + 120°) \end{aligned} \tag{3}$$

In the considered structure the optimizing block (Optimization) is optionally applied in order to improve the dynamic properties of the drive system. An application of such a block is not possible in the standard structure (Fig. 1). The considered optimization consist in correction of the angle γ by adding the angle δ depending on motor current component $I_{ph(q)}$, according to the vector diagram (Fig. 5), where the resistance of motor winding is neglected, E_f, U_{ph} are induced voltage (back EMF) and phase voltage on terminals of BLDC motor winding. As a consequence of this correction the motor current has only one component in the axis q perpendicular to the spatial vector of permanent magnet flux $\underline{\psi}_M$. The correction allows to minimize the magnitude of motor current. The output voltages of the optimizing block are obtained as a result of introducing the corrective angle δ to the dependencies (3), that describe the synchro decoder output voltages being also the input voltages of the optimizing block:

$$\begin{aligned} u_{\delta 1} &= -\,k_{TR}U_{rm}\sin(\gamma + \delta) \\ u_{\delta 2} &= -\,k_{TR}U_{rm}\sin(\gamma + \delta - 120°) \\ u_{\delta 3} &= -\,k_{TR}U_{rm}\sin(\gamma + \delta + 120°) \end{aligned} \tag{4}$$

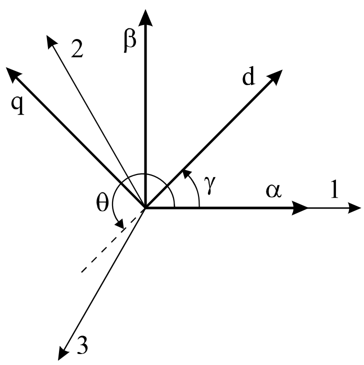

Fig. 4. The phase coordinates of motor (1,2,3), the Cartesian coordinate systems: the stationary one (0αβ) connected to the stator and the rotating one (0dq) connected to the rotor

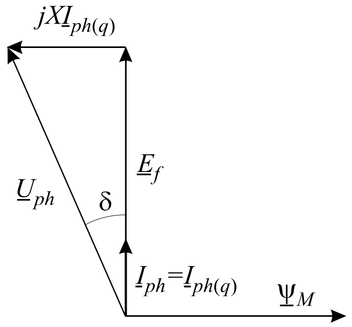

Fig. 5. The vector diagram of currents, voltages and fluxes corresponding with the applied optimization of BLDC motor control

The corrective angle δ can be introduced to the dependencies (3) using the following transformation:

$$\begin{bmatrix} u_{\delta 1} \\ u_{\delta 2} \\ u_{\delta 3} \end{bmatrix} = \frac{2}{3} \begin{bmatrix} a_1 & a_3 & a_2 \\ a_2 & a_1 & a_3 \\ a_3 & a_2 & a_1 \end{bmatrix} \begin{bmatrix} u_{d1} \\ u_{d2} \\ u_{d3} \end{bmatrix} \tag{5}$$

where:

$$\begin{bmatrix} a_1 \\ a_2 \\ a_3 \end{bmatrix} = \begin{bmatrix} \cos\delta \\ \cos(\delta - 120°) \\ \cos(\delta + 120°) \end{bmatrix} = \frac{1}{2} \begin{bmatrix} 2\cos\delta \\ -\cos\delta + \sqrt{3}\sin\delta \\ -\cos\delta - \sqrt{3}\sin\delta \end{bmatrix} \tag{6}$$

The functions $\sin\delta$ and $\cos\delta$ in dependency (6) can be expressed according to the vector diagram (Fig. 5). These functions for instantaneous values may be expressed as follows:

$$\sin\delta = \frac{Li_q}{\sqrt{L^2 i_q^2 + \psi_M^2}}, \qquad \cos\delta = \frac{\psi_M}{\sqrt{L^2 i_q^2 + \psi_M^2}} \tag{7}$$

In the abovegiven functions the following dependencies were taken into account: $E_f = \omega\Psi_{ph}$, $X = \omega L$ as well as the dependencies between modules of spatial vectors and phase variables: flux and current, in the power invariant transformation of three-phase variables to Cartesian coordinate system: $\Psi_M = (3)^{1/2}\Psi_{ph}$, $I = (3)^{1/2} I_{ph}$.

For minor values of angle $\delta < 15°$ (for the considered motor, the value of angle $\delta = 15°$ corresponds with $I \approx 3I_n$) the function $\cos\delta$ in dependency (6) may be assumed approximately as $\cos\delta \approx 1$, whereas $\sin\delta \approx \mathrm{tg}\delta \approx \delta$.

The motor current vector component i_q, required in dependencies (7), may be obtained as a result of transformation of motor phase currents to the reference frame 0dq connected to the rotor. In three-phase circuit without the neutral conductor there is no the zero component of current vector, therefore:

$$i_1 + i_2 + i_3 = 0 \tag{8}$$

Thus, for the proper operation of drive system, the measurements only two from three motor phase currents are required, whereas the third one may be obtained using the equation (8). In this case the following dependency may be used in order to calculate the motor current vector component i_q:

$$i_q = \sqrt{\frac{2}{3}} \frac{i_2(u_{d2} - u_{d1}) + i_3(u_{d3} - u_{d1})}{k_{TR} U_{rm}} \tag{9}$$

The dependencies (3) were taken into account in order to derive the dependency (9).

Results of model-simulation investigations

Time changes of motor output torque (τ_e), angular velocity (ω) and phase current (i) during reversing a BLDC motor, controlled according to the proposed strategy (Fig. 2), are shown in Figs. 6 and 7. In the model-simulation investigations the following parameters of BLDC motor were taken into account: 4 kW, 400 V, 3000 rpm (in the proposed control strategy, the BLDC motor is energized by the PWM-controlled voltage source inverter in the same manner as induction motor or synchronous motor, therefore, one pole pair is available), 11.5 A, 0.5 Ω, 9 mH, 181 V (back EMF), 0.005 kgm^2. The mathematical model of sinusoidal BLDC [9] was applied.

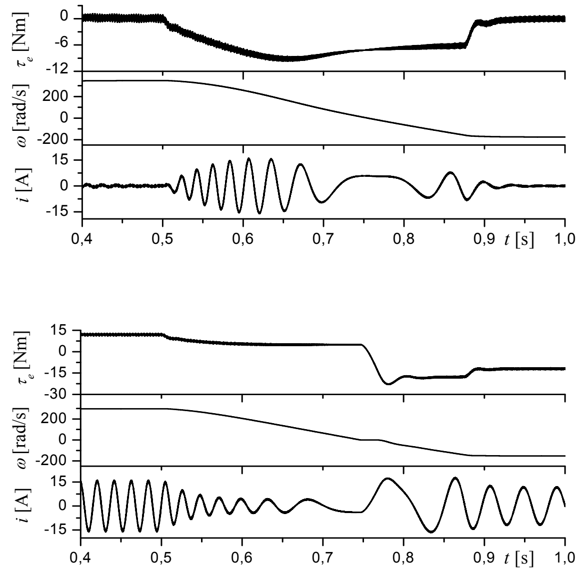

Fig. 6. Reversing the BLDC motor, controlled according to the proposed strategy (Fig. 2), without optimization (u_{ref}: $+U \rightarrow -U/2$): at the top – unloaded motor ($\tau_m = 0$), at the bottom – loaded motor ($\tau_m = \tau_n$)

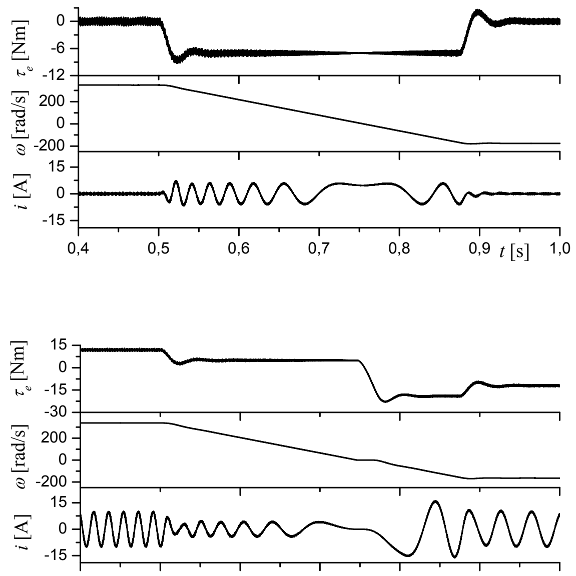

Fig. 7. Reversing the BLDC motor, controlled according to the proposed strategy (Fig. 2), with optimization (u_{ref}: $+U \rightarrow -U/2$): at the top – unloaded motor ($\tau_m = 0$), at the bottom – loaded motor ($\tau_m = \tau_n$)

Conclusions

On the basis of the presented time changes of motor variables it may be concluded that motor output torque does not contain any pulsations, whereas the high-frequency distortions of the output torque and phase currents caused by PWM-controlled voltage source inverter can also be found in the standard BLDC motor control system, however, in Fig. 1 they were omitted. The application of optimizing block in the proposed control structure allows to minimize the magnitude of motor current ($I_n \approx 7$ A) as well as the changes of motor angular velocity caused by the changes of motor load (compare the steady-state velocity of the unloaded motor $\tau_m = 0$ and the steady-state velocity of the loaded motor $\tau_m = \tau_n$, at the same voltages $u_{ref} = +U$ and $-U/2$).

REFERENCES

[1] Yedamale P., *Brushless DC (BLDC) Motor Fundamentals*, Microchip Technology Inc., U.S.A., 2003

[2] *Synchro and Resolver Engineering Handbook*, Moog Components Group Inc., Blacksburg, U.S.A., 2004

[3] Giridharan K., Chellamuthu C., Microcontroller Based Model of a Virtual BLDC Motor, *European Journal of Scientific Research*, 75 (2012) No.2, 179-192

[4] Domoracki A., Krykowski K., Silniki BLDC – klasyczne metody sterowania, *Zeszyty Problemowe Maszyny Elektryczne*, (2005), nr 72, 155-159

[5] Jąderko A., Dobór parametrów regulatora prędkości w napędzie elektrycznym z silnikiem bezszczotkowym BLDC, *Śląskie Wiadomości Elektryczne*, (2011), nr 6, 46-50

[6] Nowak M., Analiza stanów dynamicznych układu napędowego zawierającego silnik BLDC oraz długi element sprężysty, *XXIII Sympozjum Środowiskowe PTZE, Zastosowania Elektromagnetyzmu w Nowoczesnych Technikach i Medycynie*, Mikołajki, Czerwiec 2013

[7] Lis M., Algorytm obliczenia wybranych parametrów różniczkowych silnika bezszczotkowego o wzbudzeniu od magnesów trwałych o sterowaniu trapezoidalnym (BLDC), *Przegląd Elektrotechniczny*, 88 (2012), nr 9a, 116-118

[8] Lis M., Magneto-Mechanic Characteristic in the Brushless Motor with Permanent Magnet Induction and Trapezoidal Driving, *Zeszyty Problemowe Maszyny Elektryczne*, 91 (2011), nr 3, 1-4

[9] Campa R., Torres E., Salas F., Santibanez V., On Modeling and Parameter Estimation of Brushless DC Servo-actuators for Position Control Tasks, *Proceedings of the 17th World Congress The International Federation of Automatic Control*, Seoul, Korea, July 6-11, 2008, 2312-2317

***Author**: dr hab. inż. Andrzej Popenda, prof. PCz, Politechnika Częstochowska, Instytut Elektrotechniki Przemysowej, Al. Armii Krajowej 17, 42-200 Częstochowa, E-mail: popenda@el.pcz.czest.pl.*